Tumor necrosis factor receptor signaling modulates carcinogenesis in a mouse model of breast cancer

Ling He [a]; Kruttika Bhat [a]; Sara Duhacheck-Muggy [a]; Angeliki Ioannidis [a]; Le Zhang [a]; Nhan T. Nguyen [a]; Neda A. Moatamed [b,c]; Frank Pajonk [a,c,*]

[a] Department of Radiation Oncology, David Geffen School of Medicine, University of California Los Angeles, Los Angeles, CA, USA
[b] Department of Pathology and Laboratory Medicine, David Geffen School of Medicine at UCLA, Los Angeles, CA, USA
[c] Jonsson Comprehensive Cancer Center, University of California Los Angeles, Los Angeles, CA, USA

Abstract

Pro-inflammatory conditions have long been associated with mammary carcinogenesis and breast cancer progression. The underlying mechanisms are incompletely understood but signaling of pro-inflammatory cytokine TNFα through its receptors TNFR1 and TNFR2 is a major mediator of inflammation in both obesity and in the response of tissues to radiation, 2 known risk factors for the development of breast cancer. Here, we demonstrated the loss of one TNFR2 allele led to ductal hyperplasia in the mammary gland with increased numbers of mammary epithelial stem cell and terminal end buds. Furthermore, loss of one TNFR2 allele increased the incidence of breast cancer in MMTV-Wnt1 mice and resulted in tumors with a more aggressive phenotype and metastatic potential. The underlying mechanisms include a preferential activation of canonical NF-κB signaling pathway and autocrine production of TNFα. Analysis of the TCGA dataset indicated inferior overall survival for patients with down-regulated TNFR2 expression. These findings unravel the imbalances in TNFR signaling promote the development and progression of breast cancer, indicating that selective agonists of TNFR2 could potentially modulate the risk for breast cancer in high-risk populations.

Introduction

Since 1975, the incidence of breast cancer in the United States has been steadily rising. For 2019, 268,600 new cases were estimated, making up 15.2% of all new cancer cases in the United States. At the same time, 5-year survival rates increased from 75.3% to 89.9% in 2015 (https://seer.cancer. gov/statfacts/html/breast.html). Total 41,760 women in the United States are predicted to die from breast cancer in 2019 accounting for 6.9% of all cancer deaths in the country.

Major risk factors for the development of breast cancer aside from gender and age are obesity [1] and thoracic radiotherapy during puberty [2]. Both obesity and radiotherapy cause systemic or local pro-inflammatory conditions with elevated TNFα levels in adipose tissue [3] or within normal tissues exposed to radiation [4]. TNFα signals through binding to its receptors, TNFR1 (also called p55 or TNFRSF1A) and TNFR2 (p75 or TNFRSF1B), with distinct and common pathways downstream of TNFR1 and TNFR2 affecting cell death and/or survival [5].
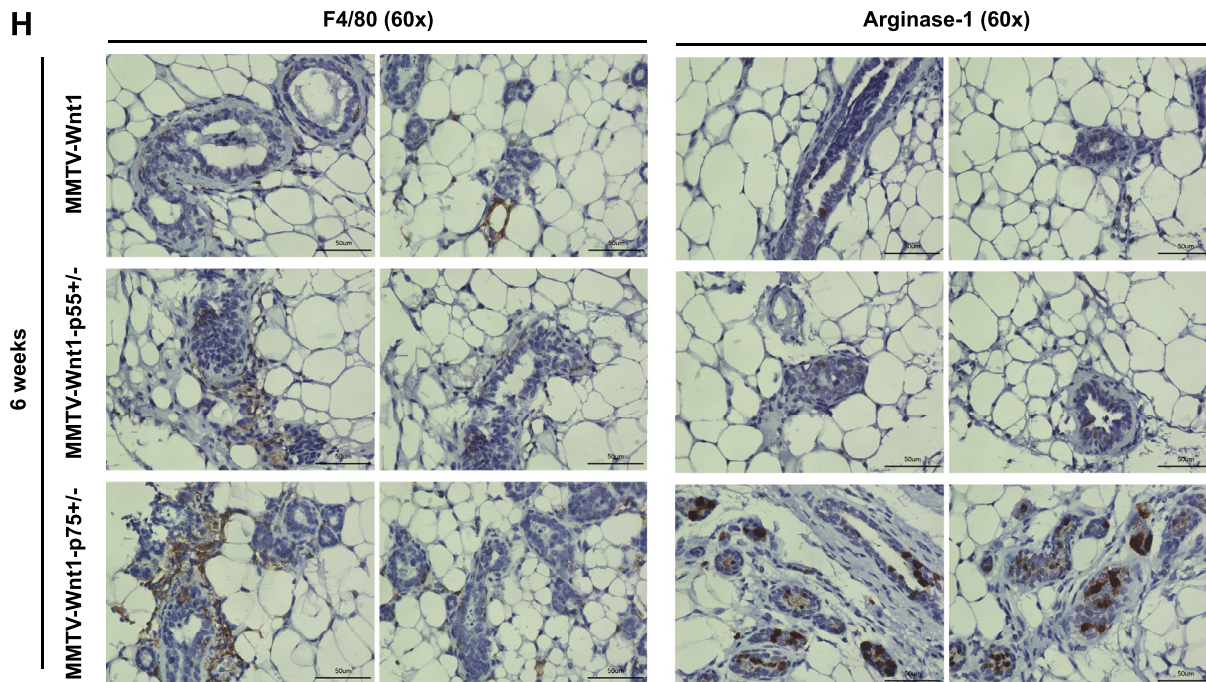
TNFα, mainly derived from activated macrophages, is a well-known pro-inflammatory cytokine that regulates the inflammatory processes in tumor development and progression [6]. High level of TNFα is associated with an aggressive behavior and a poor prognosis in many malignant cancers, including breast cancer [6,7]. In tumor cells, TNFα activates IκB kinases (IκKs), c-Jun N-terminal kinase (c-JNK), and mitogen-activated protein kinase signaling to stimulate the nuclear translocation of transcription factors including nuclear factor kappa B (NF-κB), which involves in inflammation, cellular transformation, survival, proliferation, angiogenesis, invasion, and metastasis [8]. The NF-κB family of transcription factors includes 5 members: RelA (p65), NFκB1 (p50), NFκB2 (p52), RelB, and c-Rel,

Fig. 1. TNFR1/TNFR2 imbalances affect mammary gland development. (A) #4 mammary glands were isolated from 6-wk-old female C57BL/6 wt, p55 or p75 KO mice, and mounted (LN: lymph node). (B, C) Mammary gland ductal outgrowth was quantified by measuring whole mammary gland area using ImageJ and the number of terminal end buds (TEBs) and side-buds was counted, respectively. (D) Whole mount staining of #4 mammary glands dissected from MMTV-Wnt1, MMTV-Wnt1-p55$^{+/-}$, and MMTV-Wnt1-p75$^{+/-}$ females. (E) Mammary gland ductal outgrowth was quantified by whole mammary gland area using ImageJ. (F) Mammary epithelial stem cells were isolated from 6-wk-old MMTV-Wnt1 and MMTV-Wnt1-p75$^{+/-}$ females. Mammosphere-forming capacity was evaluated after 2-wk and 3-wk mammosphere culture. (G, H) Immunohistochemistry staining of mammary gland sections from 6-wk-old MMTV-Wnt1, MMTV-Wnt1-p55$^{+/-}$, and MMTV-Wnt1-p75$^{+/-}$ mice using the macrophage markers F4/80, iNOS (M1) and Arginase-1 (M2). All experiments have been performed with at least 3 biological independent repeats. *P* values were calculated using a one-way ANOVA for B and C; un-paired student's *t* test for E and F. *P value < 0.05, **P value < 0.01, ***P value < 0.001, and ****P value < 0.0001.

which are expressed in nearly all cell types and regulate genes with different functions [9]. The activation of diverse NF-κB subunits can induce either the canonical or non-canonical NF-κB pathways, which plays distinct roles in both development of normal tissues and malignancies. Abnormal constitutive activation of NF-κB pathway has been widely reported to be associated with breast cancer development and progression [10]. However, the intracellular signaling cascades through distinct TNFRs (TNFR1 or TNFR2), specifically the NF-κB pathway have not been clearly demonstrated in the development of mammary gland and breast cancer in literature. However, recent reports indicated a specific role of TNFR2 in tumor metastasis and progression through immunosuppression [11].

In this study, we tested the hypothesis that TNFα signaling contributes to the development of breast cancer. Using a transgenic mouse model for spontaneous breast cancer development crossed with TNFR1 or TNFR2 knockout animals we demonstrated that loss of one TNFR2 allele not only affects mammary gland development, but also significantly increases the incidence of breast cancer and leads to a more aggressive tumor phenotype.

Materials and methods

Animals

MMTV-Wnt1, p55 and p75 knockout (KO) mice were originally obtained from the Jackson Laboratories (Bar Harbor, ME). All mice were re-derived, bred, and maintained in a pathogen-free environment in the American Association of Laboratory Animal Care-accredited Animal Facilities of the Department of Radiation Oncology, University of California

(Los Angeles, CA) in accordance to all local and national guidelines for the care of animals. Due to extensive ductal hyperplasia, the female MMTV-Wnt1 transgenic mice cannot lactate, so we crossed the male MMTV-Wnt1 (+) mice with female p55 KO or p75 KO mice to generate heterozygous MMTV-Wnt1-p55$^{+/-}$ and MMTV-Wnt1-p75$^{+/-}$ offspring. Genotyping was performed for the MMTV-Wnt1 transgene. Mice were monitored regularly and tumors were harvested before exceeding humane endpoints.

Whole mammary gland mounting

The mammary glands from 6-wk-old female mice were carefully excised and spread directly onto a glass slide without changing their original in situ shape. The tissue was fixed by immersing in Carnoy's fixative solution (100%EtOH, chloroform, glacial acetic acid; 6:3:1) at 4°C overnight. Glands were hydrated and stained with carmine alum overnight at room temperature. The stained tissues were then dehydrated and cleared in xylene. Images were captured and merged at 4× using a digital microscope (BZ-9000, Keyence, Itasca, IL). Ductal outgrowth was quantified by measurement of the area (mm^2) covered by the ductal tree in merged images of the mammary gland whole mounts in ImageJ and the terminal end buds (TEBs) and side-buds were counted manually in an unbiased manner.

Cell lines

The human SUM159PT breast cancer cell line was purchased from Asterand (Detroit, MI). Human MCF-7 breast cancer cell line was purchased from American Type Culture Collection (Manassas, VA).
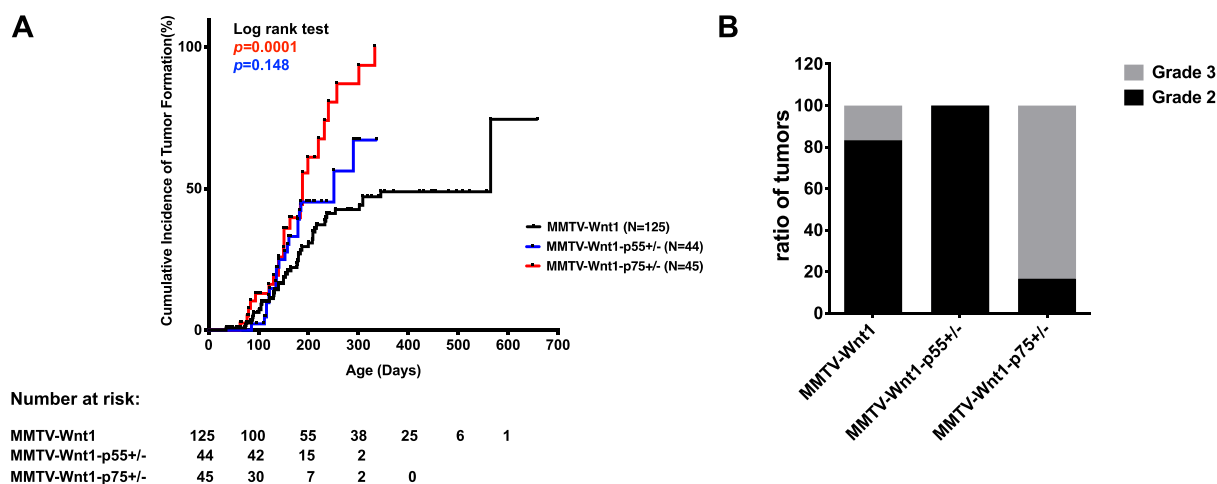
Fig. 2. Loss of one allele of TNFR2 increases BCICs and promotes tumor vasculature with greater metastatic potential. (A) Cumulative incidence curves for breast cancers in MMTV-Wnt1, MMTV-Wnt1-p55$^{+/-}$ and MMTV-Wnt1-p75$^{+/-}$ females. Breast tumors were observed and measured until they reached the study endpoint. Log-rank (Mantel-Cox) test for comparisons of Kaplan-Meier survival curves indicated significant difference between MMTV-Wnt1-p75$^{+/-}$ and MMTV-Wnt1 mice (P value = 0.0001). (B) Tumors were harvested, fixed and embedded in paraffin and cut into 4 μm sections. H&E staining was performed and the stained slides were graded blind by a clinical pathologist. (C) Representative gross view of the tumors from MMTV-Wnt1, MMTV-Wnt1-p55$^{+/-}$, and MMTV-Wnt1-p75$^{+/-}$ mice. (D) Immunohistochemistry staining of Vimentin and Snail (EMT markers) for the MMTV-Wnt1, MMTV-Wnt1-p55$^{+/-}$, and MMTV-Wnt1-p75$^{+/-}$ tumor sections. (E) qRT-PCR for EMT-related genes Vimentin, Snail and Slug in MMTV-Wnt1, MMTV-Wnt1-p55$^{+/-}$, and MMTV-Wnt1-p75$^{+/-}$ primary tumor cell lines. (F, G) Immunohistochemistry staining of Ki67 (proliferating marker) for the MMTV-Wnt1, MMTV-Wnt1-p55$^{+/-}$, and MMTV-Wnt1-p75$^{+/-}$ tumor sections, with the slides graded by clinical pathologist for the percentage of tumor cells positive for nuclear Ki67. (H, I) Migration and invasion assays of primary tumor cells isolated from MMTV-Wnt1, MMTV-Wnt1-p55$^{+/-}$, and MMTV-Wnt1-p75$^{+/-}$ mice. The migrated and invaded cell numbers were counted and quantified by ImageJ, respectively. (J) Mammosphere forming capacity of primary tumor spheres isolated from MMTV-Wnt1, MMTV-Wnt1-p55$^{+/-}$, and MMTV-Wnt1-p75$^{+/-}$ mice. The number of spheres formed was counted and calculated as a ratio to the initial number of cells plated, and then normalized to the MMTV-Wnt1 value. (K) Clonogenic assay of primary tumor cells extracted from MMTV-Wnt1, MMTV-Wnt1-p55$^{+/-}$, and MMTV-Wnt1-p75$^{+/-}$ mice. The colony number was counted and presented as the percentage relative to the initial number of cells plated. All experiments have been performed with at least 3 biological independent repeats. P values were calculated using 1-way ANOVA for E, G–K; Log-rank (Mantel-Cox) test for A. *P value < 0.05, **P value < 0.01, and ****P value < 0.0001.

SUM159PT cells were cultured in log-growth phase in F12 Medium (Invitrogen, Carlsbad, CA) supplemented with 5% fetal bovine serum, penicillin (100 units/mL), streptomycin (100 μg/mL), 5 μg/mL insulin (Eli Lilly, Indianapolis, IN), 0.1% 1M HEPES buffer (4-(2-hydroxyethyl)-1-piperazineethanesulfonic acid, Invitrogen) and 1 μg/mL hydrocortisone (Pfizer, New York, NY). MCF-7 cells were cultured in log-growth phase in Dulbecco's Modified Eagle Medium (DMEM) (Invitrogen, Carlsbad, CA) supplemented with 10% fetal bovine serum, penicillin, and streptomycin. All cells were grown in a humidified incubator at 37°C with 5% CO$_2$ and routinely tested for mycoplasma infection (MycoAlert, Lonza). The identity of the cell line was confirmed by DNA fingerprinting (Laragen, Culver City, CA).

ZsGreen-cODC expressing cells were obtained as described in [12]. Briefly, cells were infected with a lentiviral vector coding for a fusion protein between the fluorescent protein ZsGreen and the C-terminal degron of murine ornithine decarboxylase. The latter targets ZsGreen to ubiquitin-independent degradation by the 26S proteasome, thus reporting lack of proteasome function through accumulation of ZsGreen-cODC. We previously reported that cancer cell populations lacking proteasome activity are enriched for tumor-initiating cells in glioblastoma, breast cancer, and cancer of the head and neck region [12–15] and others have confirmed these findings independently in tumors of the liver, lung, cervix, pancreas, osteosarcoma, and colon [16–21]. After infection with the lentivirus, cells expressing the ZsGreen-cODC fusion protein were further selected with G418 for 5 d. Successful infection was verified using the proteasome inhibitor MG132 (Sigma, MO).

Primary breast tumor cell culture

Breast tumor tissues were extracted from MMTV-Wnt1, MMTV-Wnt1-p55$^{+/-}$, or MMTV-Wnt1-p75$^{+/-}$ female mice and washed 3 times with PBS/1% Penicillin/Streptomycin. For tumor dissociation, Miltenyi C tubes (gentleMACS C tubes, Cat # 130-093-237, Auburn, CA, USA) were preloaded with 100 μL enzyme D, 50 μL enzyme R and 12.5 μL enzyme A provided in the mouse Tumor Dissociation Kit (Cat # 130-096-730, Miltenyi, Auburn, CA) in 2.35 mL of F12 media. The breast tumor tissues were finely chopped with a scalpel and transferred into the C tubes. Tumor tissues were further dissociated by running the m_impTumor_02 program once on the gentleMACS Dissociator (Cat# 130-093-235, Miltenyi). The tubes were next placed in a shaker incubator at 37°C for 60 min. After incubation, the tubes were once again placed in the gentleMACS Dissociator and subjected twice to the same dissociation program as described above. The tubes were briefly centrifuged at 300× g to collect the digested cells at the bottom of the tube. The cells were re-suspended in the enzyme-containing medium and filtered through a 70-μm filter into a 50 mL conical tube. The filter was washed with 10 mL F12 media and centrifuged at 300× g for 7 min. The supernatant was aspirated, and the pellet was re-suspended in 2 mL of ACK lysis buffer (Cat # 10-548E, BioWhittaker, Walkersville, MD) to lyse the red blood cells. After 2 min, the conical tubes were centrifuged at 300× g for 7 min and the supernatant was aspirated. The cell pellet was resuspended in 1 to 2 mL F12 media and cell numbers were counted using a hemocytometer. Subsequently, the cells were plated onto 100 mm dishes in
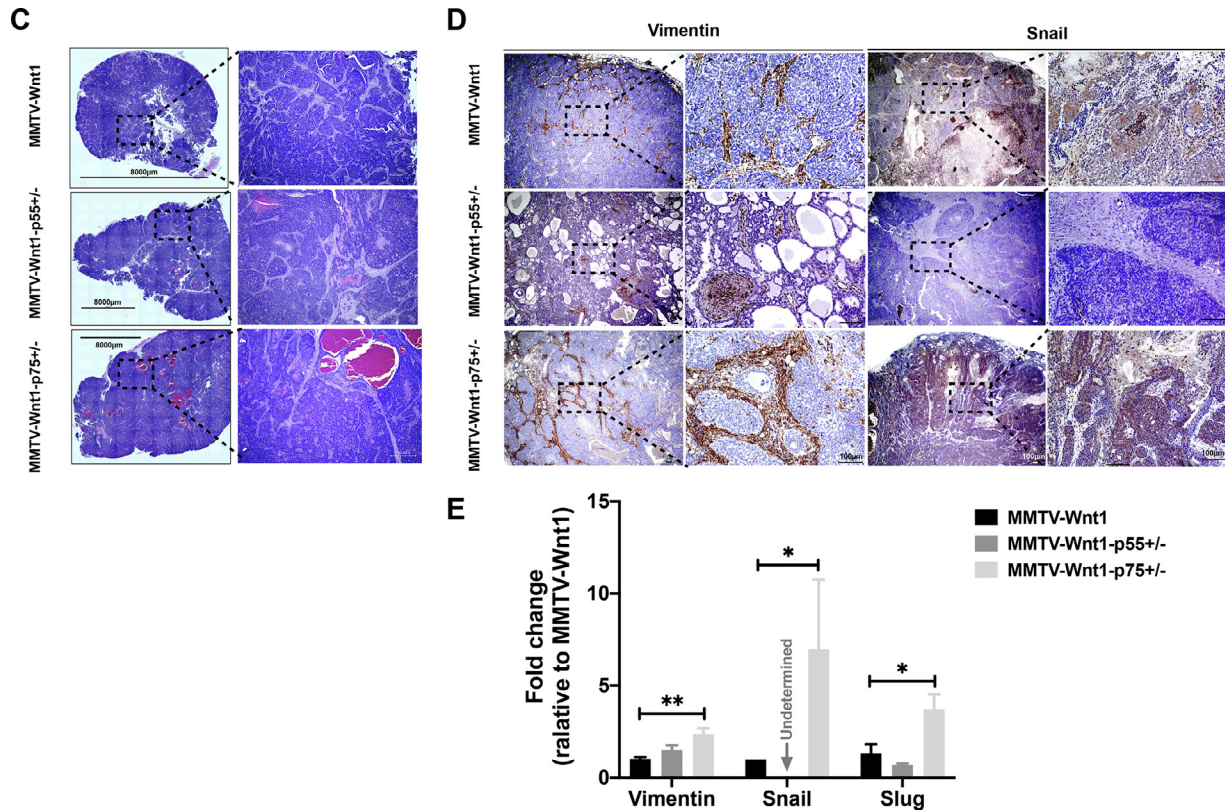
Fig. 2. Continued

SUM159PT culture medium supplemented with plasmocin and grown in a humidified incubator at 37°C with 5% CO_2.

Irradiation

Cells were irradiated at room temperature using an experimental X-ray irradiator (Gulmay Medical Inc. Atlanta, GA) at a dose rate of 5.519 Gy/min for the time required to apply a prescribed dose. The X-ray beam was operated at 300 kV and hardened using a 4 mm Be, a 3 mm Al, and a 1.5 mm Cu filter and calibrated using NIST-traceable dosimetry. Corresponding controls were sham irradiated.

In vitro limiting dilution assays

SUM159PT and MCF-7 spheres were dissociated by TrypLE and plated in mammosphere media (DMEM-F12, 10 mL/500 mL B27 [Invitrogen], 5 μg/mL bovine insulin [Sigma], 4 μg/mL heparin [Sigma], 20 ng/mL basic fibroblast growth factor [bFGF, Sigma], and 20 ng/mL epidermal growth factor [EGF, Sigma]) into 96-well ultra-low adhesion plates, ranging from 1 to 256 cells per well, along with a single dose of TNFα (1, 2.5, 5, 10, 50, 100 ng/mL) or vehicle (0.1% bovine serum albumin [BSA]), respectively. Growth factors (EGF and bFGF) were added every 3 days. The number of spheres formed per well was then counted and expressed as a percentage of the initial number of cells plated.

MMTV-Wnt1, MMTV-Wnt1-p55$^{+/-}$, and MMTV-Wnt1-p75$^{+/-}$ mammospheres were cultured from their corresponding monolayer cells. The cells were detached with Trypsin and plated in SUM159PT mammosphere media for sphere formation. The spheres were then dissociated by TrypLE and plated into 96-well ultra-low adhesion plates, ranging from 2 to 512 cells per well, along with a single dose of TNFα (1, 10, 100 ng/mL) or vehicle (0.1% BSA) applied. Growth factors (EGF and bFGF) were added every 3

d. The number of spheres formed per well was then counted, expressed as the percentage of the initial number of cells plated, and normalized to the counts in the MMTV-Wnt1 0.1% BSA-treated control group.

Clonogenic survival assay

MMTV-Wnt1, MMTV-Wnt1-p55$^{+/-}$, and MMTV-Wnt1-p75$^{+/-}$ monolayer cells were trypsinized and plated in 6-well plates at a density of 2000 cells for MMTV-Wnt1, and 200 cells for both MMTV-Wnt1-p55$^{+/-}$ and MMTV-Wnt1-p75$^{+/-}$ per well. The cell culture media was changed every 3 d. After 2 wk, the colonies were fixed and stained with 0.1% crystal violet. Colonies consisting of at least 50 cells were counted in each group and presented as percentage of the initial number of cells plated.

SUM159PT and MCF-7 monolayer cells were trypsinized and plated in 6-well plates at a density of 200 cells per well with the presence of TNFα (1, 2.5, 5, 10, 50, 100 ng/mL) or vehicle (0.1% BSA). After 2 wk, the colonies were fixed and stained with 0.1% crystal violet. Colonies consisting of at least 50 cells were counted in each group and presented as percentage of the initial number of cells plated.

Cell migration/invasion assay

Cell migration was quantified using Transwell plates (8 μm pore size; Corning). After 12 h of serum starvation, 1×10^5 MMTV-Wnt1, MMTV-Wnt1-p55$^{+/-}$, or MMTV-Wnt1-p75$^{+/-}$ primary cells were placed in the insert, with 750 μL cell culture medium containing 5% FBS as the induction medium in the lower chamber. After 16 h of incubation, unmigrated cells on the upper surface of the insert were removed with a cotton swab. Migrated cells were fixed with formalin and stained with crystal violet. Images were taken randomly on a digital microscope (BZ-9000, Keyence) with 4×
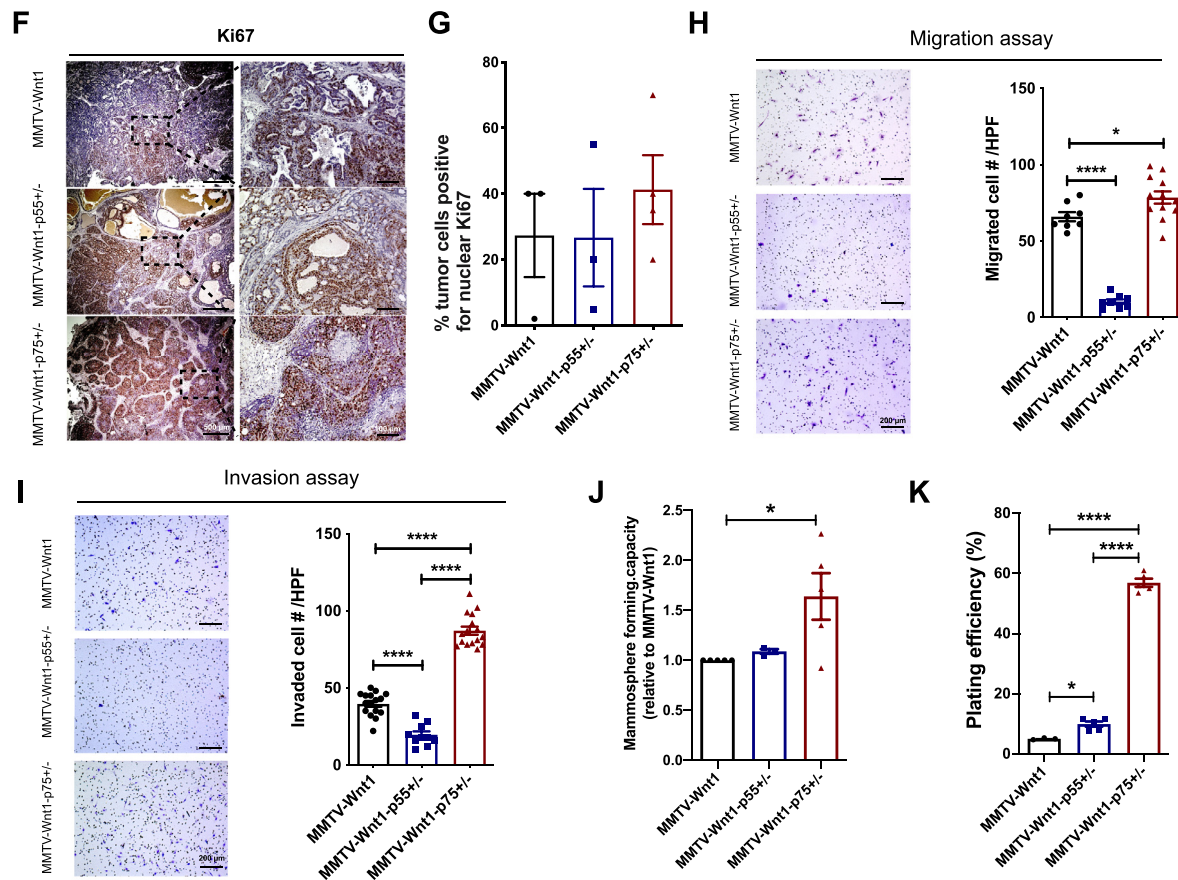
Fig. 2. Continued

magnification and the migrated cell number was counted and quantified by ImageJ.

For the cell invasion assay, 8 μm porous Transwell chamber membranes were pre-coated with 100 μL diluted Matrigel matrix solution (dilute with F12 medium to final Matrigel concentration of 200-300 μg/mL). Plates with coated invasion chambers were incubated at 37°C for 2 hours and the remaining coating buffer was removed. The cell preparation, seeding, fixation, and staining procedures were the same as the migration procedures described above. Images were randomly taken on a digital microscope and migrated cell number was counted and quantified by ImageJ.

Flow cytometry

Breast cancer-initiating cells (BCICs) were identified based on their low proteasome activity using the ZsGreen-cODC reporter system [14]. Five days after irradiation, cells were trypsinized and ZsGreen-cODC expression was assessed by flow cytometry (MACSQuant Analyzer, Miltenyi). Cells were defined as "ZsGreen-cODC positive" if the fluorescence in the FL-1H channel exceeded the level of 99.9% of the parental control cells.

Immunohistochemistry

Formalin-fixed tissue samples were embedded in paraffin and 4 μm sections were stained with hematoxylin and eosin (H&E) using standard protocols. Additional sections were baked for 1 h in an oven at 65°C, dewaxed in 2 successive Xylene baths for 5 min each and then hydrated for 5 min each using an alcohol gradient (ethanol 100%, 90%, 70%, 50%, 25%). The

slides were incubated in 3% hydrogen peroxide/methanol solution for 10 min. Antigen retrieval was performed using Heat Induced Epitope Retrieval in a citrate buffer (10 mM sodium citrate, 0.05% Tween-20, pH 6) with heating to 95°C in a steamer for 25 min. After cooling down, the slides were blocked with 10% goat serum plus 1% BSA at room temperature for 30 min and then incubated with the primary antibody against Ki67 (Abcam, Cat #15580, 1:200), Vimentin (Cell Signaling, Cat #5741S, 1:200), Snail (Abcam, Cat# 85931, 1:400), F4/80 (Cell Signaling, Cat #70076S, 1:400), iNOS (Thermo Fisher Scientific, PA1-036, 1:400) or Arginase-1 (Cell Signaling, Cat #93668S 1:400) overnight at 4°C. The next day, the slides were rinsed with PBS and then incubated with ready-to-use IHC detection reagent (Cell signaling, Danvers, MA; 10 μL) at room temperature for 1 h, rinsed, and then incubated with DAB (Cell Signaling) for 3 to 5 min. Tissues were counterstained with Harris modified Hematoxylin (Fisher scientific, Waltham, MA) for 30 s, dehydrated via an alcohol gradient (ethanol 25%, 50%, 70%, 90%, 100%) and soaked twice into Xylene. A drop of Premount mounting media (Fisher Scientific) was added on the top of each section before covering up with a coverslip.

Protein extraction and western blotting

The total protein was extracted from FACS sorted ZsGreen-cODC-negative SUM159PT cells treated with TNFα and/or irradiation. Briefly, the cells were lysed in ice-cold RIPA lysis buffer containing proteinase inhibitor (Sigma, #P8340) and phosphatase inhibitor (EMD Millipore, MA, #524629). The protein concentration in each sample was determined using the BCA protein assay (Thermo Fisher Scientific) and samples were denatured
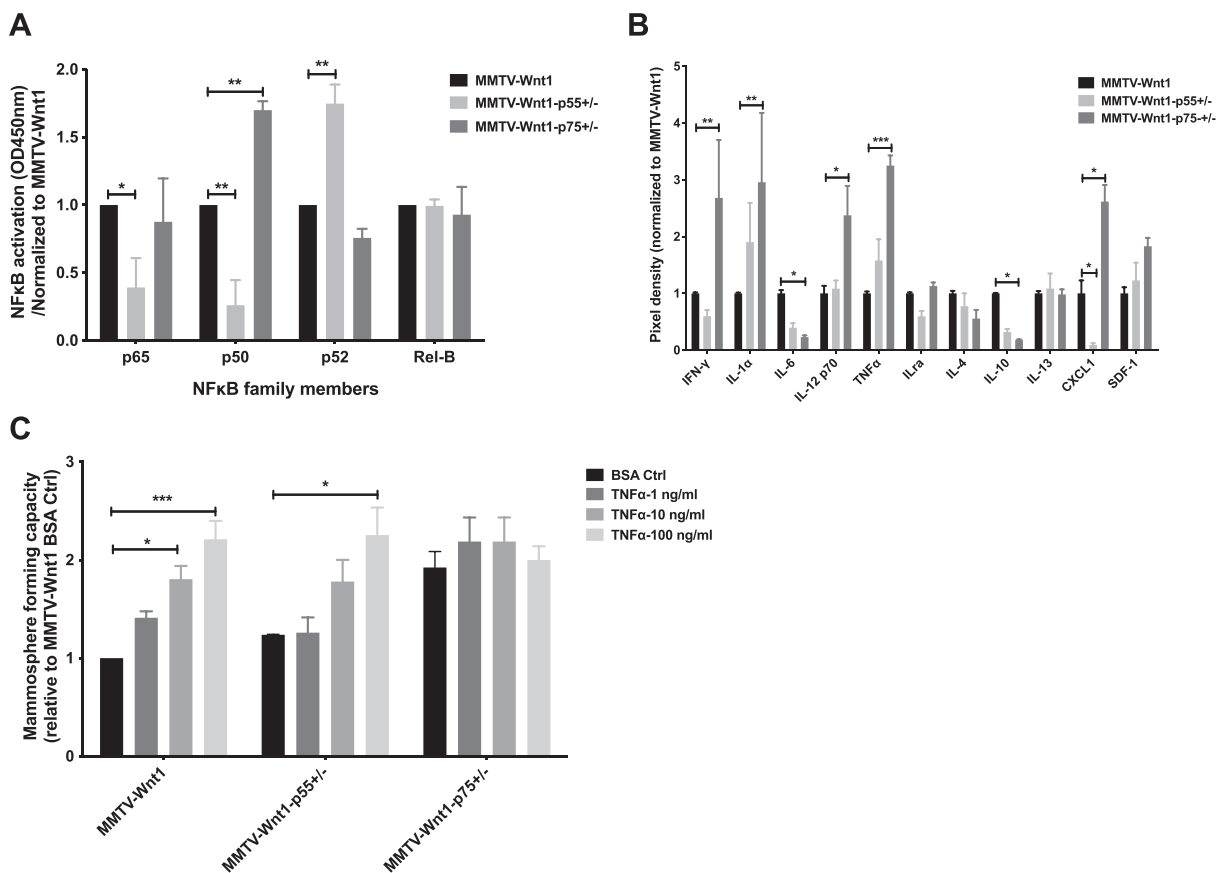
Fig. 3. Loss of 1 TNFR2 allele activates p50/NF-κB transcriptional activity with more abundant secretion of pro-inflammatory cytokines. (A) Nuclear extracts prepared from MMTV-Wnt1, MMTV-Wnt1-p55$^{+/-}$, and MMTV-Wnt1-p75$^{+/-}$ primary tumor cells were assayed at 5 μg/well for p65, p50, p52, and Rel-B activity using the Trans AM NF-κB Family Kit. The assay uses immobilized DNA-double strands with the consensus NF-κB binding motif for this transcription factor family to measure the DNA-binding activity of its subunits instead of their simple presence. Bound transcription factors are then detected using specific antibodies against the NF-κB subunits and a secondary, horseradish-peroxidase-conjugated secondary antibody. The absorbance was normalized to each subunit positive values and subsequently normalization to MMTV-Wnt1 values. (B) Proteome profiler cytokine array for nuclear extracts from MMTV-Wnt1, MMTV-Wnt1-p55$^{+/-}$, and MMTV-Wnt1-p75$^{+/-}$ primary tumor cell lines. Pixel density was analyzed and normalized to MMTV-Wnt1 by ImageJ. (C) Mammosphere-forming capacity of primary tumor spheres isolated from MMTV-Wnt1, MMTV-Wnt1-p55$^{+/-}$, and MMTV-Wnt1-p75$^{+/-}$ mice upon a single dose of TNFα (1, 10, 100 ng/mL) or vehicle (0.1% BSA) treatment. The number of spheres formed was counted, calculated as a ratio to the initial number of cells plated, and then normalized to the MMTV-Wnt1 vehicle control value. All experiments have been performed with at least 3 biological independent repeats. P values were calculated using 2-way ANOVA. $^*P$ value < 0.05, $^{**}P$ value < 0.01, and $^{***}P$ value < 0.001.

in 4X Laemmli sample buffer containing 10% β-mercapto-ethanol for 10 min at 95°C. Equal amounts of protein were loaded onto 10% SDS-PAGE gels (1X Stacking buffer - 1.0 M Tris-HCl, 0.1% SDS, pH 6.8, 1X Separating buffer - 1.5 M Tris-HCl, 0.4% SDS, pH 8.8) and were subjected to electrophoresis in 1X Running buffer (12.5 mM Tris-base, 100 mM Glycine, 0.05% SDS), initially at 40 V for 30 min followed by 80 V for 2 h. Samples were then transferred onto 0.45 μm nitrocellulose membrane (Bio-Rad) for 2 h at 80 V. Membranes were blocked in 1X TBST (20 mM Tris-base, 150 mM NaCl, 0.2% Tween-20) containing 5% BSA for 30 min and then washed with 1X TBST. These were then incubated with primary antibodies against Sox2 (Cell Signaling, Cat# 14962S, 1:1000), Oct4 (Cell Signaling, Cat # 2750S, 1:1000), Klf4 (Cell Signaling, Cat # 4038S, 1:1000), cMyc (Cell Signaling, Cat # 5605S, 1:1000) or GAPDH (Abcam, Cat# 9484, 1:1000) in 1X TBST containing 5% BSA overnight at 4°C with gentle rocking. Membranes were then washed three times for 5 min each with 1X TBST and incubated with a secondary anti-rabbit horseradish peroxidase-conjugated antibody (Cell Signaling, Cat # 7074S, 1:2000) in 5% BSA for 2 h at room

temperature with gentle rocking. Membranes were washed again 3 times for 5 min each with 1X TBST. Pierce ECL Plus Western Blotting Substrate (Thermo Fisher Scientific) was added to each membrane and incubated at room temperature for 5 min. The blots were then used to expose X-ray films (Agfa X-Ray film, VWR, Cat # 11299-020) in a dark room. GAPDH was used as a loading control. The bands that developed were scanned and their density was measured using ImageJ software. The ratio of the gene of interest over its endogenous loading control was calculated and expressed as relative intensity.

Nuclear proteins were extracted from MMTV-Wnt1, MMTV-Wnt1-p55$^{+/-}$ and MMTV-Wnt1-p75$^{+/-}$ cells. Briefly, the cells were detached and the pellet resuspended in cell lysis buffer with PMSF, DTT and protease inhibitor, incubated on ice for 20 min with intermittent tapping and inverting, then vortexed and centrifuged at 12,000× g at 4°C for 10 min. The cytoplasmic supernatant was discarded and the remaining pellet washed and resuspended in nuclear extraction buffer supplemented with PMSF, DTT, and protease inhibitor, along with 2-time sonication. The samples were
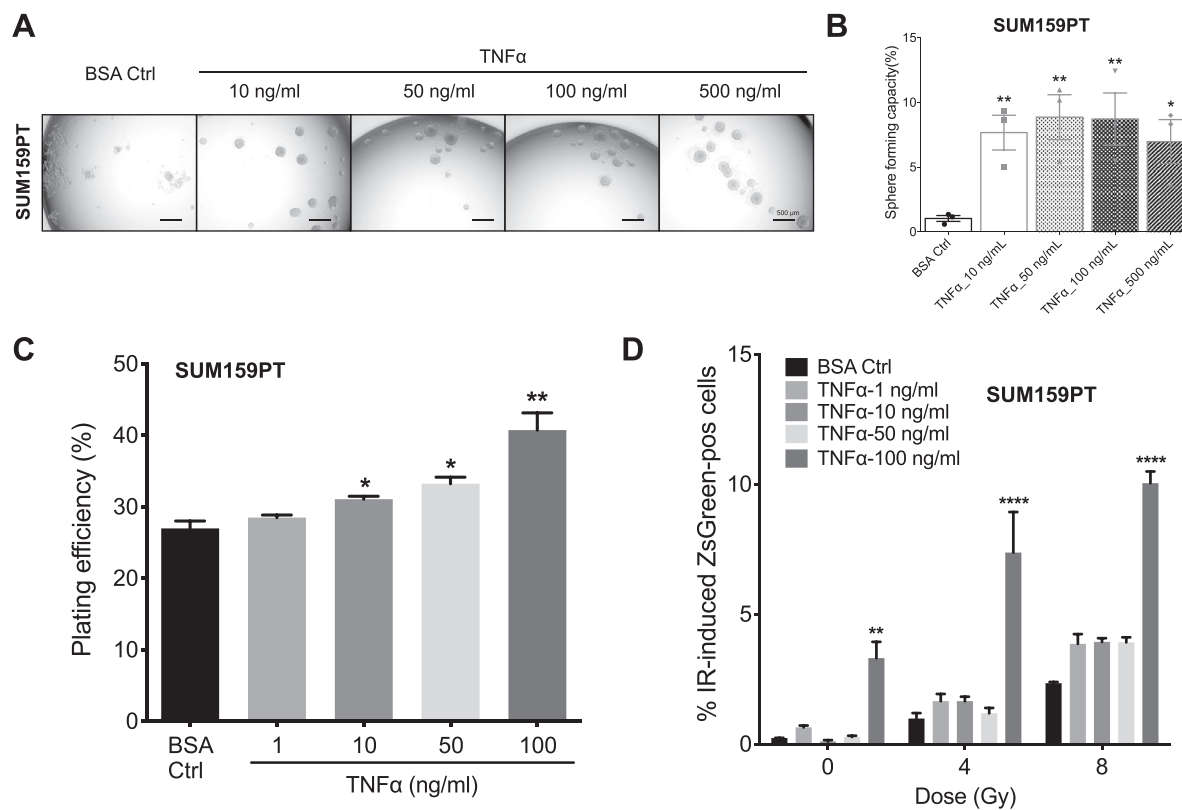
Fig. 4. TNFα increases breast cancer initiating cells and induces phenotype conversion in breast cancer cells. (A, B) Mammosphere formation assay was performed using SUM159PT mammospheres plated in a 96-well plate and treated with different concentrations of TNFα (10, 50, 100, 500 ng/mL) or vehicle (0.1% BSA). The number of mammospheres formed in each condition was counted and normalized against the vehicle control. Representative images of mammospheres in each condition (A) with the percentage of mammospheres formed (B) quantified. (C) The SUM159PT cells were plated at a density of 200 cells per well in a 6-well plate, then treated with a single dose of TNFα (1, 10, 50, 100 ng/mL) or vehicle (0.1% BSA) and cultured for 14 d. The resulting data were presented as plating efficiency with the percentage of colonies formed. (D) Sorted ZsGreen-cODC-negative SUM159PT ZsGreen-cODC vector expressing cells were plated at a density of 50,000 cells per well in a 6-well plate and the following day were pretreated with either with TNFα (1, 10, 50, 100 ng/mL) or vehicle (0.1% BSA) 1 h before irradiation at a single dose of 0, 4 or 8 Gy. Five days later, the cells were trypsinized and analyzed for ZsGreen-cODC-positive population by flow cytometry, with noninfected parental SUM159PT cells used as controls. (E) Sorted ZsGreen-cODC-negative SUM159PT cells were plated and pre-treated with 100 ng/mL TNFα or vehicle (0.1% BSA) 1 h before irradiation at a single dose of 0 or 4 or 8 Gy. The proteins were extracted 5 d later and were subjected to western blotting. The blots were analyzed for Oct4, Sox2, c-Myc, Klf4, and GAPDH, with GAPDH as the loading control. (F) The intensity of each band was quantified using ImageJ and presented as density ratio of gene over GAPDH. (G) Mammosphere formation assay were performed plating MCF-7 cells into 96-well plates, treated with different concentrations of TNFα (1, 2.5, 5, 10, 50, 100 ng/mL) or vehicle (0.1% BSA). The number of mammospheres formed in each condition was counted and quantified. (H) Sorted ZsGreen-cODC-negative MCF-7-ZsGreen-cODC cells were plated and the following day pretreated with either with TNFα (1, 2.5, 5, 10 ng/mL) or vehicle (0.1% BSA) 1 h before irradiation using a single dose of 0, 4 or 8 Gy. Five days later, the cells were trypsinized and analyzed for ZsGreen-cODC-positive cells by flow cytometry. (I, J) The MCF-7 cells were plated at a density of 200 cells per well into 6-well plates, treated with a single dose of TNFα (1, 2.5, 5, 10 ng/mL) or vehicle (0.1% BSA) and cultured for 14 d. Colony formation is shown in (I) and quantified and expressed as percentage of the number of cells pllated in (J). All experiments have been performed with at least 3 biological independent repeats. P values were calculated using 1-way ANOVA for B, C, G, and I; 2-way ANOVA for D, F, and H. *P value < 0.05, **P value < 0.01, ***P value < 0.001, and ****P value < 0.0001.

incubated on ice for 30 min, centrifuged at $12,000 \times g$ at 4°C for 15 min and the supernatant containing the nuclear proteins was transferred into fresh tubes and quantified using the BCA protein assay (Thermo Fisher Scientific).

Quantitative reverse transcription-PCR

Total RNA was isolated using TRIZOL Reagent (Invitrogen). cDNA synthesis was carried out using the SuperScript Reverse Transcription IV (Invitrogen). Quantitative PCR was performed in the QuantStudio 3 Real-Time PCR System (Applied Biosystems, Carlsbad, CA) using the PowerUp SYBR™ Green Master Mix (Applied Biosystems). C_t for each gene was determined after normalization to GAPDH and $\Delta\Delta C_t$ was

calculated relative to the designated reference sample. Gene expression values were then set equal to $2^{-\Delta\Delta C_t}$ as described by the manufacturer of the kit (Applied Biosystems). All PCR primers were synthesized by Invitrogen with GAPDH as housekeeping genes (for primer sequences see Supplementary Table 1).

NF-κB DNA-binding assay

The DNA-binding activity of NF-κB was quantified by enzyme-linked immunosorbent assay using the TransAM NF-κB family activation assay kit (Active Motif North America, Carlsbad, CA) to specifically detect and quantify the DNA-binding capacity of the NF-κB subunits p65, p50,
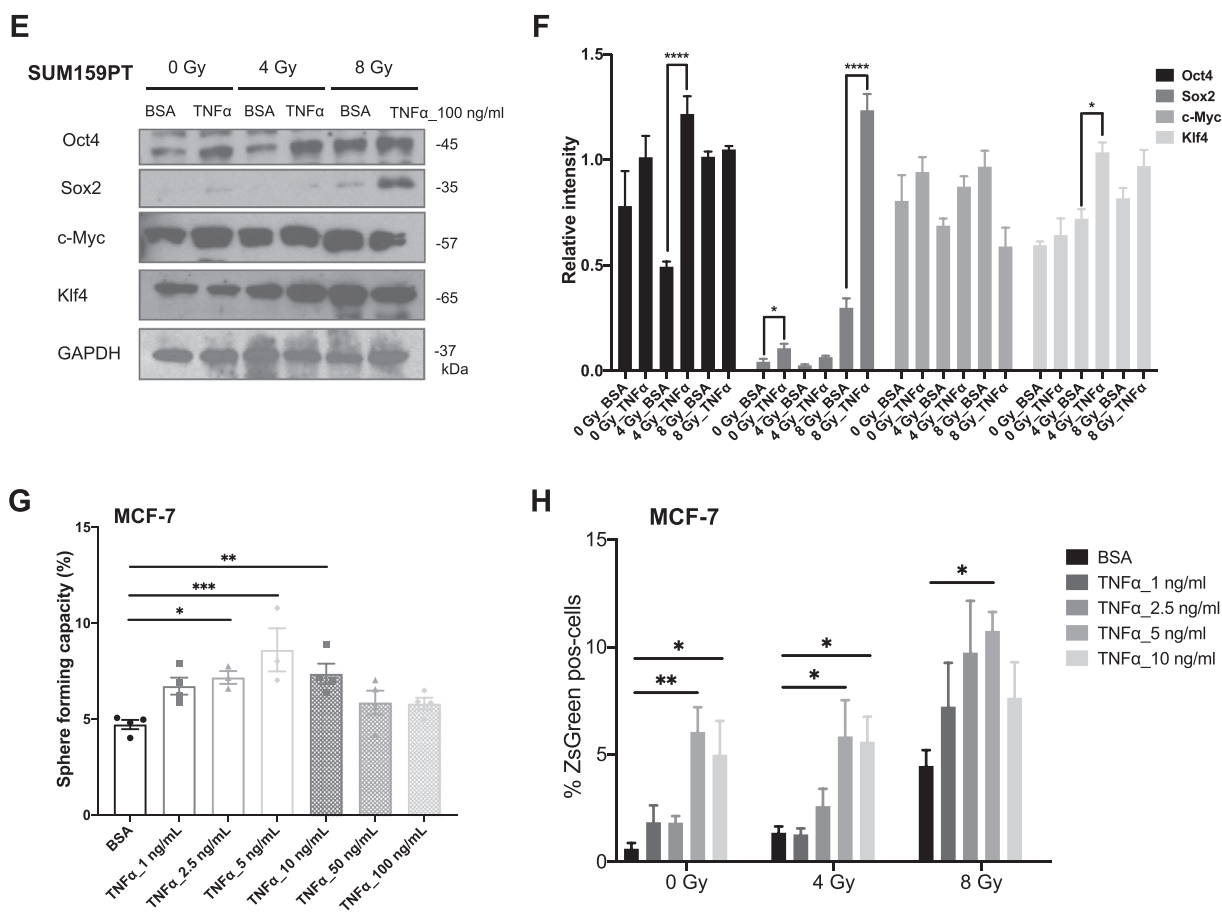
Fig. 4. Continued

p52, and Rel-B. The assay was performed according to the manufacturer's protocol and analyzed using a microplate absorbance reader (Spectramax M5, Molecular Devices, San Jose, CA).

Proteome Profiler cytokine array

The MMTV-Wnt1, MMTV-Wnt1-p55^{+/−}, and MMTV-Wnt1-p75^{+/−} primary tumor cells were plated, serum-starved overnight and placed into fresh serum-free medium the next day. Twenty-four h later, the cell culture medium was collected and centrifuged to remove insoluble materials. Secreted cytokines were measured using the Proteome Profiler Mouse Cytokine Panel A Array Kit (R&D Systems, Minneapolis, MN) according to the manufacturer's instructions. The kit consists of a nitrocellulose membrane containing 40 different anti-cytokine/chemokine antibodies spotted in duplicate. Briefly, membranes were incubated with blocking buffer at room temperature for 1 h. Cell supernatants (1 mL) were mixed with a biotinylated detection antibody cocktail at room temperature for 1 h, and then each was incubated with a membrane overnight at 4°C. The arrays were then washed 3 times for 10 min and subsequently incubated with horseradish peroxidase-conjugated streptavidin for 30 min at room temperature. The arrays were exposed to peroxidase substrate (ECL Western blotting detection reagent; Amersham Bioscience). Luminescence was detected using X-ray films, the films were scanned, and signals were quantified using the ImageJ software package. The data were normalized using the internal controls included on each array.

TCGA data mining and analysis

The Cancer Genome Atlas (TCGA) data set was accessed via the cBioPortal [22,23] and the TCGA Provisional dataset (captured December 10, 2019) was interrogated. The overall survival data and the expression data (RNA-Seq V2 RSEM Z scores for TCGA Provisional data) for TNFRSF1A and TNFRSF1B, which encode the TNFR1 and TNFR2 receptors respectively, were downloaded. Patients with both gene expression and survival data accessible were used for analysis (N = 1078). Kaplan-Meier survival analysis was performed using a Z-score cut-off of 1.0, and the patients were stratified into subgroups with over-expression, under-expression, or normal expression for each receptor. Overall survival times were used to calculate Kaplan-Meier estimates.

Statistics

All analyses were performed in the GraphPad Prism 8.0 software package. A 2-sided Student's *t* test was used for un-paired comparisons, and a 1-way or 2-way ANOVA with a post hoc Bonferroni adjustment was used for comparisons between 3 or more groups. A log-rank test was used to determine the *P* value for the Kaplan-Meier survival curves. A *P* value <0.05 was considered as statistically significant. All in vitro experiments were performed in at least 3 independent biological samples.
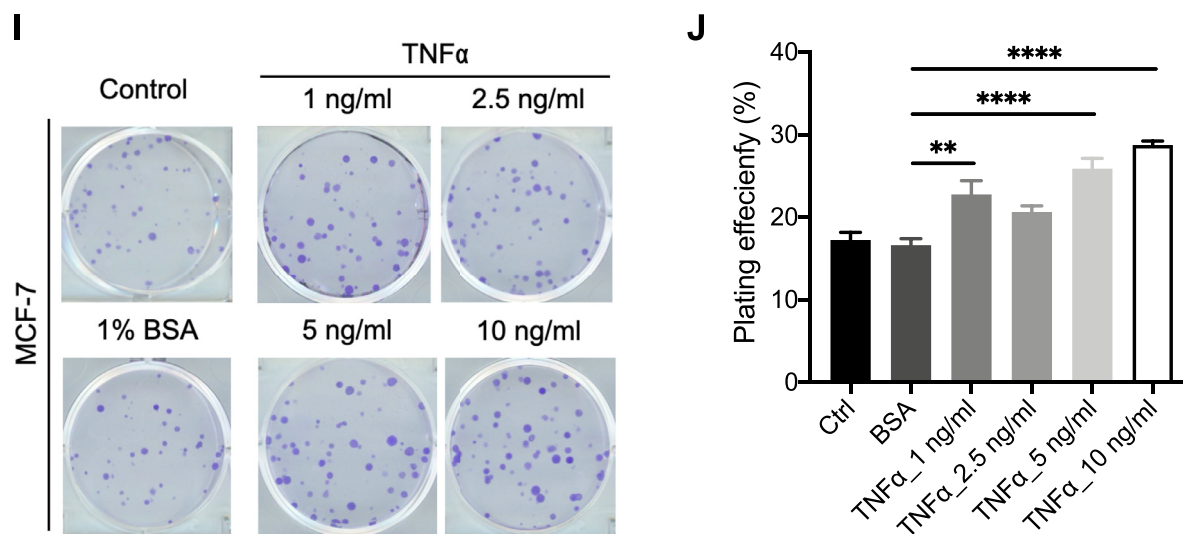
I

Control

TNFα

1 ng/ml   2.5 ng/ml

MCF-7

1% BSA   5 ng/ml   10 ng/ml

J

Fig. 4. Continued

Results

Loss of TNFR2 signaling impacts mammary gland development

In order to explore if TNFα, a major mediator of inflammation, affects the normal mammary gland development via TNFα/TNFR signaling, we utilized knockout mouse strains for the TNF receptors. Using whole mounts of the fourth mammary gland of prepubescent, 6-wk-old female C57BL/6, TNFR1 (p55) KO or TNFR2 (p75) KO animals (Figure 1A), we found a significant increase in the mammary gland area in both, p55 (3.1-fold, P value = 0.0001) and p75 (3.6-fold, P value < 0.0001) KO animals (**Figure 1B**). Compared to C57BL/6 wild-type animals, p55 KO animals had slightly decreased number of terminal end buds (TEBs), while showing a significant 2.3-fold (P value < 0.0001) increase in the number of side-buds. However, both TEBs and side-buds were significantly enriched in p75KO mice, with 3-fold (P value < 0.0001) increase in the number of TEBs and 1.8-fold (Pvalue = 0.0003) increase in side-buds (**Figure 1C**). Expression of the MMTV-Wnt1 transgene leads to robust breast cancer formation in C57BL/6 mice [24]. A comparison of the mammary gland areas between 6-wk-old C57BL/6 wild type and MMTV-Wnt1 transgenic animals showed a 1.9-fold (Pvalue = 0.0225) increase in MMT-Wnt1 animals, consistent with the published hyperproliferative phenotype of the mammary epithelium in this strain [24]. In order to test if p55 or p75 affects tumor formation under a genetic background prone to mammary carcinogenesis we next crossed MMTV-Wnt1 animals with p55 or p75 KO animals leading to animals with a hemizygous loss of the p55 or p75 gene and expression of the MMTV-Wnt1 transgene.

Mammary gland areas in MMTV-Wnt1-p75$^{+/-}$ mice were significantly larger than in MMTV-Wnt1 mice (1.7-fold, Pvalue = 0.0075; **Figure 1D/E**) but did not differ from MMTV-Wnt1-p55$^{+/-}$ mice (Pvalue = 0.429). The number of TEBs in MMTV1-Wnt1 mice was highly increased over those in wild-type mice and drastically increased in MMTV-Wnt1-p75$^{+/-}$ mice, which made their quantification impossible (**Figure 1A/D**). This suggested that hemizygous loss of either the p55 or p75 allele impacts mammary gland development when crossed with the MMTV-Wnt1 strain. In order to test for effects of the TNF receptors on the function of mammary epithelial stem cells we isolated the epithelial cells from the fat pads and subjected them to mammosphere formation assays. Mammary epithelial cells (MECs) from MMTV-Wnt1-p75$^{+/-}$ mice showed a 10.3-fold increase (Pvalue = 0.0003)

and a 6.6-fold increase (Pvalue < 0.0001) in mammosphere formation at 2 wk and 3 wk in culture respectively, when compared to MECs from MMTV-Wnt1 mice (**Figure 1F**), which is consistent with increased numbers of TEBs and indicative of increased number of mammary epithelial stem cells [25].

As macrophages are indispensable regulators for ductal outgrowth during mammary gland development, so we assessed the number of macrophages in mammary glands of 6-wk-old MMTV-Wnt1, MMTV-Wnt1-p55$^{+/-}$, or MMTV-Wnt1-p75$^{+/-}$ animals. Using the macrophage marker F4/80, the M1 activated macrophage marker iNOS and the M2 activated macrophage marker Arginase-1 we found elevated number of total macrophages as well as activated M1 and M2 macrophages associated with the mammary gland ductal system of MMTV-Wnt1-p75$^{+/-}$ mice when compared to MMTV-Wnt1 or MMTV-Wnt1-p55$^{+/-}$ animals (**Figure 1G, H**).

Loss of one TNFR2 allele accelerates breast cancer development in female MMTV-Wnt1 transgenic mice

Next, we assessed the tumor incidences in MMTV-Wnt1 mice and MMTV-Wnt1 mice crossed with p55 and p75 KO animals. Half of the female MMTV-Wnt1 mice developed mammary tumors over the course of 2 y, which was consistent with tumor incidences reported for this strain in the literature [24]. MMTV-Wnt1-p55$^{+/-}$ mice showed a slightly higher incidence of mammary tumors but this difference was not statistically significant (**Figure 2A**). However, in MMTV-Wnt1-p75$^{+/-}$ mice mammary tumors developed more rapidly with all animals showing breast tumors within the first year (Pvalue = 0.0001; **Figure 2A**). Histologically, tumors in MMTV-Wnt1 and MMTV-Wnt1-p55$^{+/-}$ mice were grade 2 breast cancers while tumors in MMTV-Wnt1-p75$^{+/-}$ mice were less differentiated and predominantly grade 3 carcinomas (**Figure 2B**). Furthermore, tumors from MMTV-Wnt1-p75$^{+/-}$ mice showed higher degrees of vascularization (**Figure 2C**), as well as the epithelial-mesenchymal transition (EMT) markers Vimentin and Snail (**Figure 2D**). In order to test if EMT markers originated from tumor cells and not only from cancer-associated fibroblasts, we assessed EMT-related gene expression levels in primary tumor cell lines established from the tumors. In accordance with the immunohistochemistry staining, the MMTV-Wnt1-p75$^{+/-}$ tumor cell lines showed significantly enhanced Vimentin, Snail, and Slug expression levels when compared to MMTV-Wnt1 cell lines, thus indicating increased EMT in MMTV-Wnt1-p75$^{+/-}$ tumors (**Figure 2E**). Interestingly, Snail was barely detected in MMTV-Wnt1-p55$^{+/-}$

tumor cell lines, which was in line with the minimal signal observed after immunohistochemistry staining. Furthermore, grading of the tumor sections by a clinical breast cancer pathologist showed a trend for increased numbers of proliferating tumor cells positive for nuclear Ki67 in MMTV-Wnt1-p75$^{+/-}$ tumors (**Figure 2F/G**).

Next, we validated the more aggressive phenotype of tumors in MMTV-Wnt1-p75$^{+/-}$ mice using a functional trans-well assay. A comparison of tumor cells from breast cancer lines established from tumors of MMTV-Wnt1, MMTV-Wnt1-p55$^{+/-}$ or MMTV-Wnt1-p75$^{+/-}$ mice revealed higher migration and invasion capacity in lines established from MMTV-Wnt1-p75$^{+/-}$ breast cancers (**Figure 2H/I**). Furthermore, cells derived from MMTV-Wnt1-p75$^{+/-}$ tumors exhibited increased mammosphere formation (**Figure 2J**) and clonogenic plating efficiency (**Figure 2K**) when compared to both MMTV-Wnt1 and MMTV-Wnt1-p55$^{+/-}$ cell lines, thus indicating higher numbers of BCICs and clonogenic cells, respectively.

Loss of one TNFR2 allele activates canonical NF-κB signaling

To gain insight into the mechanisms of how knockout of one p75 allele affects mammary gland development and breast carcinogenesis, we next compared the DNA-binding activity of NF-κB family subunits among the primary tumor cell lines using an ELISA-based assay. Nuclear extracts from MMTV-Wnt1-p75$^{+/-}$ cell lines exhibited significantly higher activation of the p50 NF-κB subunit than MMTV-Wnt1 cell lines, while the MMTV-Wnt1-p55$^{+/-}$ cell lines had higher activity of the p52 NF-κB subunit and reduced activity of p65 and p50 subunits (**Figure 3A**). Together this suggested preferential signaling through the canonical NF-κB signaling pathway in MMTV-Wnt1-p75$^{+/-}$ cell lines.

To further explore the activation of the canonical NF-κB signaling pathway in MMTV-Wnt1-p75$^{+/-}$ cell lines, we next assessed its pro-inflammatory downstream targets [26,27] using cytokine arrays. Compared to MMTV-Wnt1-derived lines, MMTV-Wnt1-p75$^{+/-}$ cell lines showed more abundant secretion of pro-inflammatory cytokines IFN-γ (2.68-fold, Pvalue = 0.0097), IL-1α (2.96-fold, Pvalue = 0.0023), TNFα (3.25-fold, Pvalue = 0.0004), and IL-12 p70 (2.37-fold, Pvalue = 0.0393), while the anti-inflammatory cytokine IL-10 (0.19-fold, Pvalue = 0.0409) was significantly diminished (**Figure 3B**). Consistent with increased migratory capacity and increased expression of EMT markers, the level of the chemotaxis-related chemokine CXCL1 was increased in MMTV-Wnt1-p75$^{+/-}$ cell lines (2.62-fold, Pvalue = 0.0133, **Figure 3B**).

Finding 3-fold increase of tumor-derived TNFα secretion in MMTV-Wnt1-p75$^{+/-}$ cell lines, we next explored the effects of exogenous TNFα ligand on self-renewal capacity of MMTV-Wnt1, MMTV-Wnt1-p55$^{+/-}$ and MMTV-Wnt1-p75$^{+/-}$ tumor cell lines. Using mammosphere formation assay, we observed a significant increase in mammosphere formation in response to TNFα treatment in MMTV-Wnt1 and MMTV-Wnt1-p55$^{+/-}$ cell lines, suggesting TNFα could promote self-renewal capacity in breast cancer cells (**Figure 3C**). However, this effect of TNFα was not notable in MMTV-Wnt1-p75$^{+/-}$ cell lines.

TNFα-induces phenotype conversion in human breast cancer cells

Next, we sought to test the effects of TNFα on both SUM159PT human triple-negative and MCF-7 human luminal breast cancer cells. Treatment with TNFα caused a significant increase in mammosphere formation suggesting that self-renewal in breast cancer cells is regulated by TNFα (**Figure 4A/B and G**). This effect of TNFα extended to an increased plating efficiency in a classic clonogenic survival assay (**Figure 4C/I**). We had previously reported that irradiation of nontumorigenic breast cancer cells led to the induction of a BCIC phenotype [13]. Using a reporter system that marks BCICs through accumulation of the fluorescent protein ZsGreen [12,14,28] we removed preexisting BCICs by FACS and irradiated

the remaining non-BCICs with 0, 4 or 8 Gy in the presence or absence of TNFα. After 5 d in culture, we observed a radiation-induced phenotype conversion of non-BCICs into induced BCICs and an amplification of this effect in the presence of TNFα (**Figure 4D/H**). This phenotype conversion correlated with the induction of the Yamanaka transcription factors Oct4, Sox2, and Klf4 (**Figure 4E/F**), which can be used to reprogram somatic cells into induced pluripotent stem cells (iPSCs) [29].
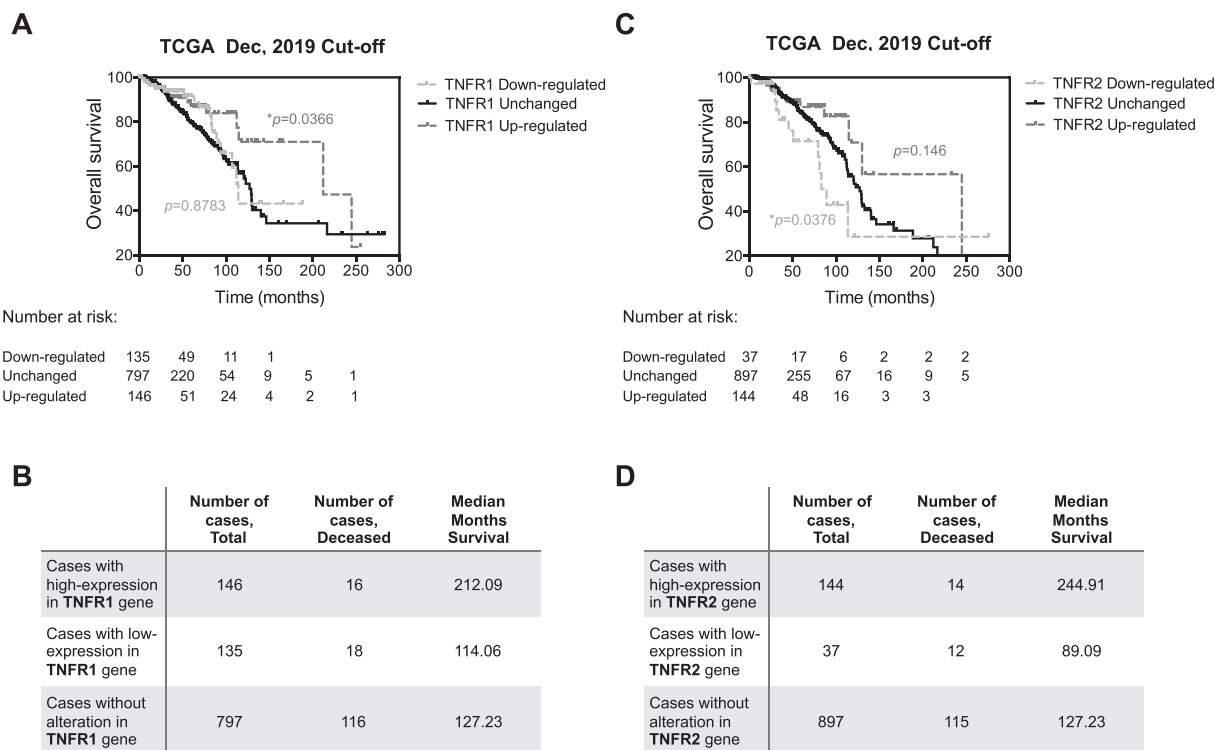
Down-regulated TNFR2 expression is associated with decreased overall survival in breast cancer patients

To further investigate whether TNFR expression is associated with the clinical outcome of breast cancer patients, we analyzed overall survival data from 1078 breast cancer patients in the TCGA Provisional dataset, stratified into subgroups with up-, down-regulated or unchanged expression of TNFR1 and 2 using a Z-score cut-off of 1.0. The median survival of patients in the subgroup with up-regulated TNFR1 expression was significantly higher (211.09 months, Pvalue = 0.0366) than that of patients in the subgroup with normal expression (127.23 months), while the median survival of patients with down-regulated TNFR1 expression was 114.06 months (Pvalue = 0.8783; **Figure 5A/B**). On the contrary, patients with down-regulated expression of TNFR2 showed an inferior median overall survival 89.09 months when compared to the median survival of 127.23 months for patients with normal receptor expression (Pvalue = 0.0376). The median survival of patients with upregulated TNFR2 expression was 244.91 months, but this was not statistically significant (Pvalue = 0.146) when compared to the median survival of patients with normal receptor expression (**Figure 5C/D**).

Discussion

Pro-inflammatory conditions are in large part driven by TNFα and have long been known to promote the development of malignancies including breast cancer [30,31]. In tumors, TNFα plays a critical role in proliferation, angiogenesis, invasion and metastasis via signaling through the TNFα/NF-κB axis [32]. However, it has been unclear, which signaling events downstream of TNFα receptors affect tumorigenesis.

In this study, we show that the homozygous knockout of either TNFR1 or TNFR2 alone increased the mammary epithelial stem cell numbers and led to accelerated prepubescent mammary gland development with hyperplastic ductal outgrowth and larger gland areas when compared to age-matched C57BL/6 wild-type animals. However, with over the past 20 years of breeding p55 and p75 KO animals we have never observed an increase in spontaneous breast cancer in either of the TNFR knock-out strains, consistent with the resistance of their genetic C57BL/6 background strain against spontaneous breast cancer development [33]. When p75 or p55 knock-out animals were crossed with MMTV-Wnt1 transgenic animals to study the effects of TNF receptors on spontaneous breast carcinogenesis, MMTV-Wnt1-p75$^{+/-}$ animals not only exhibited enhanced ductal outgrowth and greater mammary gland area, but also showed increased numbers of total, and both, M1 and M2 macrophages. Macrophages were associated with mammary epithelial cells, consistent with the important role of the microenvironment in ductal outgrowth. Our study did not investigate if hemizygous loss of p55 or p75 in the absence of the MMTV-Wnt1 transgene affects mammary gland development and this needs to be explored in future studies. Furthermore, in the litters of TNFR2 KO mice that were crossed with MMTV-Wnt1 transgenic animals, prone to develop mammary tumors [24], the onset of breast cancer was significantly accelerated and the tumors showed a more aggressive phenotype. This was also reflected in increased numbers of Ki67-, Vimentin- and Snail-positive cells. Vimentin-positive cells were primarily located at the invasive front of the tumors. In contrast, Snail-positive cells were located in the core of the tumors and were almost completely absent in

A

TCGA Dec, 2019 Cut-off

- TNFR1 Down-regulated
- TNFR1 Unchanged
- TNFR1 Up-regulated

$*p=0.0366$

$p=0.8783$

Overall survival (y-axis: 20, 40, 60, 80, 100)
Time (months) (x-axis: 0, 50, 100, 150, 200, 250, 300)

Number at risk:

Down-regulated	135	49	11	1		
Unchanged	797	220	54	9	5	1
Up-regulated	146	51	24	4	2	1

C

TCGA Dec, 2019 Cut-off

- TNFR2 Down-regulated
- TNFR2 Unchanged
- TNFR2 Up-regulated

$p=0.146$

$*p=0.0376$

Overall survival (y-axis: 20, 40, 60, 80, 100)
Time (months) (x-axis: 0, 50, 100, 150, 200, 250, 300)

Number at risk:

Down-regulated	37	17	6	2	2	2
Unchanged	897	255	67	16	9	5
Up-regulated	144	48	16	3	3	

B

	Number of cases, Total	Number of cases, Deceased	Median Months Survival
Cases with high-expression in **TNFR1** gene	146	16	212.09
Cases with low-expression in **TNFR1** gene	135	18	114.06
Cases without alteration in **TNFR1** gene	797	116	127.23

D

	Number of cases, Total	Number of cases, Deceased	Median Months Survival
Cases with high-expression in **TNFR2** gene	144	14	244.91
Cases with low-expression in **TNFR2** gene	37	12	89.09
Cases without alteration in **TNFR2** gene	897	115	127.23

Fig. 5. Overall survival evaluation of TNFR1 and TNFR2 signature in TCGA breast cancer patients. (A) The overall survival (OS) in breast cancer patients from TCGA stratified by TNFR1 mRNA expression. The light gray dotted line indicates patients with down-regulated expression of TNFR1, the dark gray dotted line represents the patients with up-regulated TNFR1 expression and the black line represents the unchanged population. OS in TNFR1 up-regulated subgroup was significantly better than that of the unchanged group (log rank test, P value $= 0.0366$). (B) The total case number, the deceased case number and the median survival of patients with down-regulated, unchanged or up-regulated TNFR1 expression. (C) OS in breast cancer patients from TCGA stratified by TNFR2 mRNA expression. The light gray dotted line indicates patients with down-regulated expression of TNFR2, the dark gray dotted line represents the patients with up-regulated TNFR2 expression and the black line represents the unchanged population. OS in TNFR2 down-regulated subgroup was significantly worse than that of the unchanged group (log rank test, P value $= 0.0376$). The number of patients at risk is listed below the Kaplan-Meier curves. (D) The total case number, the deceased case number, and the median survival time of patients with down-regulated, unchanged, or up-regulated TNFR2 expression. P values were calculated using Log-rank (Mantel-Cox) test. $*P$ value < 0.05.

tumors from MMTV-Wnt1-p55$^{+/-}$ mice, consistent with a less aggressive phenotype. Previous reports demonstrated TNFα-induced EMT via Snail [34,35], an important transcriptional repressor of E-cadherin. Loss of E-cadherin is a hallmark of EMT during which epithelial cells lose their polarity, cell-cell adhesion, epithelial characteristics and acquire migratory and invasive mesenchymal properties. The absence of Snail in tumors from MMTV-Wnt1-p55$^{+/-}$ mice suggested a possible role of TNFR2 but not TNFR1 in TNFα/Snail axis of EMT.

Compared to less aggressive tumors developing in MMTV-Wnt1 animals, tumors in MMTV-Wnt1-p75$^{+/-}$ animals showed elevated DNA-binding capacity of the NF-κB subunit p50, which indicated a preferential response of these tumors to TNFα and Interleukine-1 (IL-1) through NF-κB p50/p50 homodimers and the canonical NF-κB signaling pathway. In contrast, tumors in MMTV-Wnt1-p55$^{+/-}$ animals showed elevated DNA-binding capacity of the NF-κB subunit p52, which signals through the noncanonical NF-κB pathway, does not respond to TNFα, and exclusively depends on IKKα but not IKKβ and IKKγ [36].

Consistent with an activation of the canonical NF-κB signaling pathway, tumor cell lines derived from MMTV-Wnt1-p75$^{+/-}$ mammary tumors showed significantly upregulated levels of the pro-inflammatory cytokines IFN-γ, IL-1α, TNFα, IL-12 and the chemotaxis-related CXCL1 chemokine. Treatment of tumor cell lines derived from MMTV-Wnt1 and MMTV-Wnt1-p55$^{+/-}$ breast tumors as well as the triple-negative human breast cancer

line SUM159PT with exogenous TNFα led to a dose-dependent increase in mammosphere formation and also an increased plating efficacy in the colony-forming assays. On the contrary, tumor cell lines derived from MMTV-Wnt1-p75$^{+/-}$ breast tumors did not respond to TNFα but showed higher baseline mammosphere formation comparable to that of MMTV-Wnt1 and MMTV-Wnt1-p55$^{+/-}$ cell lines stimulated with high concentrations of TNFα, results consistent with an autocrine pro-inflammatory loop. It is noteworthy that when BCICs were purged from SUM159PT cells as described previously [14], treatment with TNFα or radiation led to re-expression of the developmental transcription factors Oct4, Sox2, and Klf4 and that coincided with a phenotype conversion in some of the remaining non-BCICs into induced BCICs. The combined treatment with radiation and a high concentration of TNFα appeared to have an additive effect. These finding were in line with our previous report on radiation-induced phenotype conversion in breast cancer [13]. Inflammatory breast cancer is a rare and aggressive form of the disease with worse survival than other types of breast cancer [37]. Our observation of TNFα-induced phenotype conversion could be one aspect of the aggressive phenotype of inflammatory breast cancer.

Finally, we analyzed the overall survival of 1078 breast cancer patients in the TCGA Provisional dataset. Patients with upregulated TNFR1 expression showed significantly increased overall survival while patients with down-regulated TNFR2 expression had a significantly reduced overall survival, thus supporting the clinical significance of our experimental findings. A shortfall

of our study is that the TCGA data are based on gene expression changes in the bulk tumor material. However, while this material will certainly also contain mRNA from immune cells, one can assume that those changes in TNFR1 and TNFR2 expression primarily reflect expression changes in tumors cells, indicating a role for TNFR signaling imbalances in modulating the aggressiveness of breast cancer cells directly and not necessarily though immunomodulation alone. Future studies should employ single cell or single nuclei RNA-Sequencing to further clarify this question.

We are not the first to report an effect of TNFα on the mammary gland. TNFα has been shown to increase the growth of both normal and malignant mammary epithelial cells in experimental models [38,39] and has been associated with tumorigenesis by affecting stem cell fate and inducing the transformation of normal stem cells [40,41]. TNFα exerts its activity by stimulation of its receptors TNFR1 and TNFR2. These 2 receptors trigger distinct and common signaling pathways that control cell apoptosis and survival [5]. However, to our best knowledge, the effects of imbalances in TNFR1 and TNFR2 signaling on mammary gland development and carcinogenesis have never been studied as per the literature.

In our present study, we elucidated the role of TNFRs in mammary gland development and carcinogenesis using genetic mouse models. While expression of the MMTV-Wnt1 transgene in our model was restricted to the mammary epithelium, TNFRs were knocked out globally, suggesting that the effects observed were not just from the changes in the mammary epithelium and the tumor cells derived from it or the surrounding microenvironment, but could also have rather also accounted for systemic changes of immunity and inflammation. By testing the effects of TNFα on mammary epithelial cells and mammary tumor cells derived from our different mouse strains in vitro we were able to separate these effects, demonstrating a clear role for TNFα in the self-renewal of normal mammary epithelial stem cells as well as BCICs.

Macrophages are important regulators of mammary gland developmental processes, especially during puberty stage when they are recruited to the neck region of the TEBs and guide the mammary gland ducts out-branching [42]. Furthermore, macrophages are mediators of inflammation, play an indispensable role in modulating innate immune responses and interacting as tumor-associated macrophages with the surrounding microenvironment [43]. However, the effects of both the resident macrophages and the tumor-associated macrophages on tumorigenesis or progression are still incompletely understood. In our present study, we did not perform longitudinal studies to address whether macrophages were responsible for increased ductal outgrowth and numbers of TEBs or if instead TNFR signaling imbalances in epithelial cells were the primary cause for this phenotype with macrophages secondarily associating with the ductal system. Future studies are warranted to address these outstanding questions.

Conclusions

We conclude that the roles of TNFR1 and TNFR2 in breast cancer development and progression are rather complex and go far beyond the pro-inflammatory properties of TNFα. It still needs to be determined if selective targeting of the receptors by e.g., specific TNFR2 agonists or TNFα inhibitors [44–46] can modulate mammary carcinogenesis and disease progression.

Availability of data and materials

All data and methods are included in the manuscript. Tumor-derived cell lines will be made available from the corresponding author upon reasonable request.

Author contributions

Funding

Conflict of interest

The authors declare no competing interests.

Supplementary materials

Supplementary material associated with this article can be found, in the online version, at doi:10.1016/j.neo.2020.12.007.

References

[1] Jiralerspong S, Goodwin PJ. Obesity and breast cancer prognosis: evidence, challenges, and opportunities. *J Clin Oncol* 2016;**34**:4203–16.

[2] Travis LB, Hill D, Dores GM, Gospodarowicz M, van Leeuwen FE, Holowaty E, Glimelius B, Andersson M, Pukkala E, Lynch CF, et al. Cumulative absolute breast cancer risk for young women treated for Hodgkin lymphoma. *J Natl Cancer Inst* 2005;**97**:1428–37.

[3] Hotamisligil GS, Spiegelman BM. Tumor necrosis factor alpha: a key component of the obesity-diabetes link. *Diabetes* 1994;**43**:1271–8.

[4] Chiang CS, McBride WH. Radiation enhances tumor necrosis factor alpha production by murine brain cells. *Brain Res* 1991;**566**:265–9.

[5] Wajant H, Siegmund D. TNFR1 and TNFR2 in the control of the life and death balance of macrophages. *Front Cell Dev Biol* 2019;**7**:91.

[6] Balkwill F. Tumour necrosis factor and cancer. *Nat Rev Cancer* 2009;**9**:361–71.

[7] Miles DW, Happerfield LC, Naylor MS, Bobrow LG, Rubens RD, Balkwill FR. Expression of tumour necrosis factor (TNF alpha) and its receptors in benign and malignant breast tissue. *Int J Cancer* 1994;**56**:777–82.

[8] Hagemann T, Wilson J, Kulbe H, Li NF, Leinster DA, Charles K, Klemm F, Pukrop T, Binder C, Balkwill FR. Macrophages induce invasiveness of epithelial cancer cells via NF-kappa B and JNK. *J Immunol* 2005;**175**:1197–205.

[9] Ghosh S, May MJ, Kopp EB. NF-kappa B and Rel proteins: evolutionarily conserved mediators of immune responses. *Annu Rev Immunol* 1998;**16**:225–60.

[10] Wang W, Nag SA, Zhang R. Targeting the NFkappaB signaling pathways for breast cancer prevention and therapy. *Curr Med Chem* 2015;**22**:264–89.

[11] Sheng Y, Li F, Qin Z. TNF receptor 2 makes tumor necrosis factor a friend of tumors. *Front Immunol* 2018;**9**:1170.

[12] Vlashi E, Kim K, Lagadec C, Donna LD, McDonald JT, Eghbali M, Sayre JW, Stefani E, McBride W, Pajonk F. In vivo imaging, tracking, and targeting of cancer stem cells. *J Natl Cancer Inst* 2009;**101**:350–9.

[13] Lagadec C, Vlashi E, Della Donna L, Dekmezian C, Pajonk F. Radiation-induced reprogramming of breast cancer cells. *Stem Cells* 2012;**30**:833–44.

[14] Bhat K, Sandler K, Duhachek-Muggy S, Alli C, Cheng F, Moatamed NA, Magyar CE, Du L, Li G, McCloskey S, et al. Serum erythropoietin levels, breast cancer and breast cancer-initiating cells. *Breast Cancer Res* 2019;**21**:17.

[15] Lagadec C, Vlashi E, Bhuta S, Lai C, Mischel P, Werner M, Henke M, Pajonk F. Tumor cells with low proteasome subunit expression predict overall survival in head and neck cancer patients. *BMC Cancer* 2014;**14**:152.

[16] Muramatsu S, Tanaka S, Mogushi K, Adikrisna R, Aihara A, Ban D, Ochiai T, Irie T, Kudo A, Nakamura N, et al. Visualization of stem cell features in human hepatocellular carcinoma reveals in vivo significance of tumor-host interaction and clinical course. *Hepatology* 2013;**58**:218–28.

[17] Pan J, Zhang Q, Wang Y, You M. 26S proteasome activity is down-regulated in lung cancer stem-like cells propagated in vitro. *PLoS One* 2010;**5**:e13298.

[18] Hayashi K, Tamari K, Ishii H, Konno M, Nishida N, Kawamoto K, Koseki J, Fukusumi T, Kano Y, Nishikawa S, et al. Visualization and characterization of cancer stem-like cells in cervical cancer. *Int J Oncol* 2014;**45**:2468–74.

[19] Adikrisna R, Tanaka S, Muramatsu S, Aihara A, Ban D, Ochiai T, Irie T, Kudo A, Nakamura N, Yamaoka S, et al. Identification of pancreatic cancer stem cells and selective toxicity of chemotherapeutic agents. *Gastroenterology* 2012;**143**:234–45 e237.

[20] Tamari K, Hayashi K, Ishii H, Kano Y, Konno M, Kawamoto K, Nishida N, Koseki J, Fukusumi T, Hasegawa S, et al. Identification of chemoradiation-resistant osteosarcoma stem cells using an imaging system for proteasome activity. *Int J Oncol* 2014;**45**:2349–54.

[21] Qian Y, Wu X, Yokoyama Y, Okuzaki D, Taguchi M, Hirose H, Wang J, Hata T, Inoue A, Hiraki M, et al. E-cadherin-Fc chimera protein matrix enhances cancer stem-like properties and induces mesenchymal features in colon cancer cells. *Cancer Sci* 2019;**110**:3520–32.

[22] Cerami E, Gao J, Dogrusoz U, Gross BE, Sumer SO, Aksoy BA, Jacobsen A, Byrne CJ, Heuer ML, Larsson E, et al. The cBio cancer genomics portal: an open platform for exploring multidimensional cancer genomics data. *Cancer Discov* 2012;**2**:401–4.

[23] Gao J, Aksoy BA, Dogrusoz U, Dresdner G, Gross B, Sumer SO, Sun Y, Jacobsen A, Sinha R, Larsson E, et al. Integrative analysis of complex cancer genomics and clinical profiles using the cBioPortal. *Sci Signal* 2013;**6**:pl1.

[24] Li Y, Hively WP, Varmus HE. Use of MMTV-Wnt-1 transgenic mice for studying the genetic basis of breast cancer. *Oncogene* 2000;**19**:1002–9.

[25] Bandyopadhyay A, Dong Q, Sun LZ. Stem/progenitor cells in murine mammary gland: isolation and functional characterization. *Methods Mol Biol* 2012;**879**:179–93.

[26] Lawrence T. The nuclear factor NF-kappa B pathway in inflammation. *Cold Spring Harb Perspect Biol* 2009;**1**:a001651.

[27] Hoesel B, Schmid JA. The complexity of NF-kappa B signaling in inflammation and cancer. *Mol Cancer* 2013;**12**:86.

[28] Duhachek-Muggy S, Bhat K, Medina P, Cheng F, He L, Alli C, Saki M, Muthukrishnan SD, Ruffenach G, Eghbali M, et al. Radiation mitigation of the intestinal acute radiation injury in mice by 1-[(4-nitrophenyl)sulfonyl]-4-phenylpiperazine. *Stem Cells Transl Med* 2020;**9**:106–19.

[29] Yamanaka S, Blau HM. Nuclear reprogramming to a pluripotent state by three approaches. *Nature* 2010;**465**:704–12.

[30] Coussens LM, Werb Z. Inflammation and cancer. *Nature* 2002;**420**:860–7.

[31] Grivennikov SI, Greten FR, Karin M. Immunity, inflammation, and cancer. *Cell* 2010;**140**:883–99.

[32] Ham B, Fernandez MC, D'Costa Z, Brodt P. The diverse roles of the TNF axis in cancer progression and metastasis. *Trends Cancer Res* 2016;**11**:1–27.

[33] Medina D. Of mice and women: a short history of mouse mammary cancer research with an emphasis on the paradigms inspired by the transplantation method. *Cold Spring Harb Perspect Biol* 2010;**2**:a004523.

[34] Wang H, Wang HS, Zhou BH, Li CL, Zhang F, Wang XF, Zhang G, Bu XZ, Cai SH, Du J. Epithelial-mesenchymal transition (EMT) induced by TNF-alpha requires AKT/GSK-3beta-mediated stabilization of snail in colorectal cancer. *PLoS One* 2013;**8**:e56664.

[35] Wang Y, Zhou BP. Epithelial-mesenchymal transition in breast cancer progression and metastasis. *Chin J Cancer* 2011;**30**:603–11.

[36] Oeckinghaus A, Ghosh S. The NF-kappa B family of transcription factors and its regulation. *Cold Spring Harb Perspect Biol* 2009;**1**:a000034.

[37] Menta A, Fouad TM, Lucci A, Le-Petross H, Stauder MC, Woodward WA, Ueno NT, Lim B. Inflammatory breast cancer: what to know about this unique, aggressive breast cancer. *Surg Clin North Am* 2018;**98**:787–800.

[38] Varela LM, Ip MM. Tumor necrosis factor-alpha: a multifunctional regulator of mammary gland development. *Endocrinology* 1996;**137**:4915–24.

[39] Warren MA, Shoemaker SF, Shealy DJ, Bshar W, Ip MM. Tumor necrosis factor deficiency inhibits mammary tumorigenesis and a tumor necrosis factor neutralizing antibody decreases mammary tumor growth in neu/erbB2 transgenic mice. *Mol Cancer Ther* 2009;**8**:2655–63.

[40] Wang L, Zhao Y, Liu Y, Akiyama K, Chen C, Qu C, Jin Y, Shi S. IFN-gamma and TNF-alpha synergistically induce mesenchymal stem cell impairment and tumorigenesis via NF kappa B signaling. *Stem cells* 2013;**31**:1383–95.

[41] Afify SM, Seno M. Conversion of stem cells to cancer stem cells: undercurrent of cancer initiation. *Cancers (Basel)* 2019;**11**:345.

[42] Gouon-Evans V, Lin EY, Pollard JW. Requirement of macrophages and eosinophils and their cytokines/chemokines for mammary gland development. *Breast Cancer Res* 2002;**4**:155–64.

[43] DeNardo DG, Coussens LM. Inflammation and breast cancer. Balancing immune response: crosstalk between adaptive and innate immune cells during breast cancer progression. *Breast Cancer Res* 2007;**9**:212.

[44] Leung CH, Zhong HJ, Yang H, Cheng Z, Chan DS, Ma VP, Abagyan R, Wong CY, Ma DL. A metal-based inhibitor of tumor necrosis factor-alpha. *Angew Chem Int Ed Engl* 2012;**51**:9010–14.

[45] Mercogliano MF, Bruni S, Elizalde PV, Schillaci R. Tumor necrosis factor alpha blockade: an opportunity to tackle breast cancer. *Front Oncol* 2020;**10**:584.

[46] Kang TS, Mao Z, Ng CT, Wang M, Wang W, Wang C, Lee SM, Wang Y, Leung CH, Ma DL. Identification of an iridium (III)-based inhibitor of tumor necrosis factor-alpha. *J Med Chem* 2016;**59**:4026–31.